Transformative Approach to Investigate the Microphysical Factors Influencing the Airborne Transmission of Pathogens

Mara Otero Fernandez,[1] Richard J. Thomas,[2] Henry Oswin,[1]

Allen E. Haddrell,[1,#] Jonathan P. Reid[1,#]

[1] School of Chemistry, University of Bristol, Bristol, BS8 1TS, UK

[2] Defence Science Technology Laboratory (DSTL), Porton Down, Salisbury, SP4 0JQ, UK

 # Corresponding authors: Dr. Allen E. Haddrell, a.haddrell@bristol.ac.uk; Prof. Jonathan P. Reid, j.p.reid@bristol.ac.uk.

Running Title: Microphysical factors influencing airborne bacteria

Keywords: atmospheric bioaerosols, bacterial viability, electrodynamic balance

ABSTRACT

Emerging outbreaks of airborne pathogenic infections worldwide, such as the current SARS-CoV-2 pandemic, have raised the need to understand parameters affecting the airborne survival of microbes in order to develop measures for effective infection control. We report a novel experimental strategy, TAMBAS (Tandem Approach for Microphysical and Biological Assessment of Airborne Microorganisms Survival), to explore the synergistic interactions between the physicochemical and biological processes that impact airborne microbe survival in aerosol droplets. This innovative approach provides a unique and detailed understanding of the processes taking place from aerosol droplet generation through to equilibration and viability decay in the local environment, elucidating decay mechanisms not previously described. The impact of evaporation kinetics, solute hygroscopicity

and concentration, particle morphology and equilibrium particle size on airborne survival are reported, using *Escherichia coli* (MRE162) as a benchmark system. For this system, we report that the particle crystallisation does not directly impact microbe longevity, bacteria act as crystallization nuclei during droplet drying and equilibration, and the kinetics of size and compositional change appear to have a larger effect on microbe longevity than equilibrium solute concentration.

IMPORTANCE

A transformative approach to identify the physicochemical processes that impact the biological decay rates of bacteria in aerosol droplets is described. It is shown that the evaporation process and changes in the phase and morphology of the aerosol particle during evaporation impact microorganism viability. The equilibrium droplet size was found to affect airborne bacterial viability. Furthermore, the presence of *Escherichia coli* (MRE162) in a droplet does not affect aerosol growth/evaporation, but influences the dynamic behaviour of the aerosol through processing the culture media prior to aerosolization affecting the hygroscopicity of the culture medium; this highlights the importance of the inorganic and organic chemical composition within the aerosolised droplets that impact hygroscopicity. Bacteria act also as a crystallisation nucleus. The novel approach and data has implications for increased mechanistic understanding of aerosol survival and infectivity in bioaerosol studies spanning medical, veterinary, farming, and agricultural fields, including the role of micro-organisms in atmospheric processing and cloud formation.

1. INTRODUCTION

Transmission of respiratory infectious diseases via the airborne route has been identified as the major transmission mode in many epidemics, predominantly in indoor environments.(1–6) Nevertheless, the mechanisms that control the survival of airborne respiratory pathogens remain largely unknown due to the complex multifactorial processes which are involved.(7) Further investigation is critical to determine the fundamental mechanisms of airborne disease transmission, necessary not only to

develop strategies to mitigate the impact of disease outbreaks, but also to understand seasonality of infectious diseases,(8) improve treatment of respiratory infections(9) and even determine synergistic effects of air pollution on the atmospheric microbial community.(10)

Some of the critical factors that are thought to affect microbial survival in the aerosol phase include relative humidity (RH), temperature, particle size and microbial load.(11–19) Further, experimental methods of aerosol generation (i.e. reflux nebulizers) and sampling (i.e. impingement) can introduce damage to microorganisms. Thus, the aerosolised population may not be wholly representative of microorganisms aerosolised naturally through a cough or sneeze. (20–24) However, the CELEBS system minimises damage imparted during aerosol generation and sampling meaning biological decay is purely due to the environment and droplet conditions. (25)

To address the fundamental mechanistic questions central to understanding airborne disease transmission, we present a new approach derived from using two complementary experimental tools. First, the aerosol droplet evaporation kinetics, changes in particle morphology during drying and changes in the solute hygroscopicity are fully quantified using a comparative kinetic electrodynamic balance (CK-EDB), providing a detailed understanding of the dynamic behaviour of aerosol particles.(26, 27) Second, the bioaerosol survival rates as a function of time, particle composition and environmental conditions, of identical particle types are measured with a Controlled Electrodynamic Levitation and Extraction of Bioaerosol onto a Substrate (CELEBS).(25) When used in combination, these particle levitation technologies can be used to interrogate the true airborne state of airborne microorganisms. Understanding this state is critical since the physicochemical conditions that microorganisms are exposed to within an aerosol host droplet can differ dramatically from those in a bulk phase sample,(28) potentially impacting their viability and consequently, their transmissibility between hosts. Combining the strengths of these complementary methodologies for probing aerosol particles directly, the TAMBAS approach enables an exploration of the complex interconnections between airborne microphysics and biological decay.

2. RESULTS

The capability of our novel approach, described in the *Methods* section (after the references below) and *Supplementary Information*, is assessed through combined measurements of the dynamics driving the evolving size, composition, morphology, and hygroscopic response with their corresponding biological outcome. We illustrate the value of this approach by reporting outcomes of studies to explore the coupling of aerosol microphysical and biological processes using *Escherichia coli* (MRE162) as a benchmark system, representing the survival rates as a decline in culturability as it is described in the *Methods* section.

2.1 The Water Content of Microbiological Media: Bacterial Processing of Growth Media Affects Aerosol Hygroscopicity

The retrieval of equilibrium hygroscopic properties of microbial media from mass-transfer kinetics measurements was performed in the CK-EDB.(26, 29) The relationship between water activity and aerosol composition for common microbial media are compared to thermodynamic model predictions for NaCl (E-AIM,(30) Fig. 1). Freshly autoclaved LB broth and LB broth previously used to culture bacteria over 24h with subsequent withdraw of *E. coli* MRE-162 cells, are referred to as non-metabolized and metabolized, respectively. The hygroscopic growth curves in Fig. 1 show that PBS has similar hygroscopicity to NaCl alone (NaCl makes up 83% of the mass of PBS). However, both LB broth solutions, with 60% of the solute mass arising from organic components, are much less hygroscopic. Interestingly, non-metabolized and metabolized LB broth display different hygroscopicity, suggesting that the metabolization of LB broth by bacteria alters the solute composition and, thus, the water content of aerosol droplets at a particular RH. Although it is well known that bacteria alters composition of media through metabolism, the effect that this has on aerosol hygroscopicity is a novel observation. Ostensibly, microbes affect the physicochemical properties of bioaerosol altering the initial solute composition.

In these studies, the microbial media used to generate aerosol droplets to investigate compositional changes as a function of the ambient RH are not representative of respiratory droplets responsible for, for example, human-human transmission mechanisms. However, this investigation allows us to correlate droplet compositions of different characteristics (e.g. nutrient rich such as LB broth compared to nutrient poor such as PBS) and investigate whether components play a role in the airborne survival of microorganisms. In addition, aerobiological studies have been performed since the late 1950s (31) by using different microorganism in a wide variety of suspending fluids, from water, (32) growth media, (17, 33) and PBS (34) to more representative biological compositions such as artificial saliva. (35, 36). However, most studies do not directly compare within a single study and therefore understanding the effect of composition is still largely unknown.

2.2 Changes in Phase/Morphology and Solute Concentration During Droplet Evaporation at Varying RH Affect Microorganism Viability

The evaporation profiles (including changes in morphology) of non-metabolized individual LB broth droplets (Fig. 2a) and PBS droplets (Fig. 2b) into RHs of 30%, 50% and 70% have been investigated. For evaporating LB broth solution droplets, the light scattering analysis(37) suggests the formation of NaCl inclusions (NaCl makes up 40% of the mass of LB broth) during evaporation into RHs of 30 and 50% while complete homogeneity is sustained when evaporating at 70% RH (Fig. 2a). The PBS solution droplets remain homogenous during evaporation into RHs of 50 % and above, but crystal formation is observed when evaporating at an RH of 30% (red point in Fig. 2b); at this RH, the determination of the size of the crystallised non-spherical particle is not possible.(27) As expected, the efflorescence of PBS took place between 30 and 50% RH which agrees with the known efflorescence RH for NaCl (45-50%).(38) In both Fig 2a and 2b, the morphology analysis is most certain after the droplets reach equilibrium with their environment, i.e. once the cumulative phase functions become consistent making the phase identification more robust.

To further explore the morphologies formed from the drying of PBS and LB broth droplets at 30% RH, particles were captured for SEM (scanning electron microscopy) analysis (Fig. 2c and 2d). The morphologies are as expected from the light scattering analysis performed in the CK-EDB measurements. Briefly, LB broth particles are broadly spherical in shape (Fig. 2c and Supplementary Fig. S4a) with clear evidence of dendritic salt inclusions, reflecting the likely diffusional limitation due to elevated particle viscosity of these organic-rich droplets formed on rapid drying as inclusions form (60% mfs of organic compounds).(39),(40) By contrast, PBS droplets form multiple crystals (Fig. 2d and Supplementary Fig. S4c) as the droplet rapidly dries with multiple nucleation events occurring as the solute concentration surpasses critical supersaturation for efflorescence.(41)

The rapid changes in particle size and water content during drying lead to conditions in the aerosol phase that are not accessible in the bulk liquid (e.g. supersaturated solute, high salt concentrations, ultra-viscous and even glassy states) for nearly all ambient conditions when the RH falls below 70%, potentially impacting the longevity of enclosed microorganisms. (28, 42–45) In Fig. 2e and Fig. 2f, the time-dependent changes in solute concentrations accompanying evaporation of non-metabolized LB broth and PBS droplets into gas-phases of 30, 50, 70 and 90% RHs are compared. The dynamics for these solution droplets are simulated using a quasi-steady evaporation model that accounts for the interplay of mass and heat transport during drying and is benchmarked against the experimental measurements.(46)

The impacts on E. *coli* MRE162 survival of the interconnected changes in size, particle morphology and solute concentrations taking place during evaporation of PBS and LB broth droplets at 300 s are reported in Fig. 2g and 2h. Bacterial survival is reported as the ability of a bacterium to form a colony (colony forming unit, CFU) after suspension, collection and 24 hr incubation. Overall, an inverse correlation between the final equilibrated solute concentration and *E. coli* MRE162 survival is observed.

At high RHs (90-70%), where all droplets remain homogeneous during evaporation for both droplet compositions, bacteria survival shows a significant decrease in LB broth droplets with decrease in RH, potentially due to the high solute concentration at 70%. In the case of PBS droplet composition, the reduction in survival with RH is moderate. When comparing LB broth and PBS compositions, there was not a significant difference between survival over this range of RHs. However, a higher survival at 70% RH (Fig. 2h) is reported in PBS droplets, possibly due to the higher mass of water, larger droplet size and lower solute concentration when achieving equilibrium with the gas-phase composition (c.f. Supplementary Figs. S6 and S7).

Under the driest conditions (50 to 30% RH), a significant decline in E. *coli* MRE162 survival is observed in PBS droplets (Fig. 2h) compared with a smaller decrease for LB broth droplets (Fig. 2g). This sudden reduction in survival in PBS coincides with a transition in particle phase, in this case from homogenous droplets to salt crystals (Fig. 2b and 2d). Comparing droplet compositions, a statistically significant difference survival was observed at 50% RH, also matching a difference in droplet morphologies between composition, showing a lower survivability in LB broth droplets where inclusions where observed in contrast with the homogeneity of the PBS droplets (Fig 2a c.f. 2b). Conversely, the survival reported in LB broth droplets at 30% RH is marginally higher than for PBS, likely due to the presence of organic components in LB broth which potentially enhances survival (Fig. 2h c.f. Fig. 2h).

2.3 No loss of Viability is Observed during the Rapid Drying Phase of Bioaerosol Droplets; Bacteria Act as a Crystallization Nuclei

Time-dependent measurements of the viability for *E. coli* MRE162 enclosed in LB broth and PBS droplets equilibrated at various RHs were performed over 1h (Fig. 3). Due to the gentle aerosolization processes and high-resolution sampling achieved with CELEBS, the CFUs observed for the shortest survival measurements (<5s suspension time) agree with the estimated microbial concentrations in the

droplets. This expected concentration is estimated from the cell concentration in the suspension loaded into the droplet-on-demand generator (DoD), described with a Gaussian distribution when cell concentrations are in the order of 10^8 cells mL^{-1}. The efficiency of the sequence of processes (biological sample solution to aerosol droplet creation to aerosol droplet sampling/recovery) has been discussed in detail in our previous work. (25) Thus, only the biological decay processes occurring in the aerosol phase need be considered.

Little decline in biological viability over a timescale of 5 s is observed at any of the droplet compositions and RHs. This holds even for the very rapid evaporation and equilibration time at the lowest RHs (e.g. Supplementary Fig. S6a and S7a) where the evaporative cooling and rise in solute concentration at the droplet surface can be expected to be most severe. Thus, the dynamic processes taking place (e.g. water evaporation, surface cooling, rapid changes in size and solute composition) seem to not immediately impact *E. coli* MRE162 survival. The lack of impact of the dynamics occurring during evaporation can be contrasted with current assumptions whereby two different decay constants have been reported, suggested as arising from a rapid initial decay attributed to the drying process and subsequent slower secondary phase associated with oxidative stress and the effect of environmental conditions. (11–13, 47–50) These studies were performed by using reflux atomization for aerosol generation and various methodologies for particle suspension such as the rotating drum and the static and dynamic storage chambers. (11, 13, 47, 48, 50).

The marginal decay observed up to5 s (Fig 3a and 3b) suggests that previous reports of a rapid initial loss of viability (with decay constants of 1 sec) (48)(13) are likely not occurring in the aerosol phase, but may be a systematic artefact of the aerosolization process used, since many aerosol generators impact the structural integrity of microorganisms when nebulised.(22, 23) Further, the disturbance in gas-phase conditions produced by the cumulative mass of water introduced to the system by the cloud of droplets from nebulizers is often not contemplated and, therefore, the conditions studied are not often precisely reported during droplet evaporation (tens of minutes may be necessary for the droplet

cloud to reach equilibrium).(51) The ability to determine microbial decay during dynamic microphysical processes in the aerosol phase is unique to TAMBAS approach.

The time for the first decay is apparent in Fig. 3 and is considerably longer that the time required for the droplets to reach thermodynamic equilibrium, a time that is dependent on RH. Interestingly, a significant decrease in airborne bacteria viability (compared to 5s measurement) is observed only at the lowest RHs (30 and 50%) for droplets composed of PBS during the first 60 s of suspension (*p-values* of 0.00004 and 0.00015 respectively). In contrast, the loss of viability was significant only at the highest RHs (70 and 90%) (*p-values* of 0.0013 and 0.0001 respectively) in the case of LB broth droplets. This general trend describing greater survivability in PBS droplet composition at high RHs is maintained at longer timescales. Thus, no significant decay is observed at 90% RH after 1h suspensions for droplets composed of PBS (*p-values* of 0.2) while the reduction on viability is significant for droplets with LB broth composition (*p-values* of 0.00005). This divergence in survival in droplets of different compositions may be a result of the higher solute hygroscopicity of OBS, linked to greater water content in the droplets and lower solute concentrations (Fig. S6b c.f. S7b).

Interestingly, the structure of bacteria containing PBS particles dried at 30% RH observed in the SEM analysis show *E. coli* MRE162 cells embedded in the salt crystals, coinciding with a considerably increase in the overall number of crystals when compared with pure PBS droplets (c.f. Fig. 2d with 3d and Supplementary Fig. S4c with S4d), consistent with bacteria acting as crystallization nuclei. Conversely, little change in the phase behaviour of LB broth is observed when containing bacteria (c.f. Fig. 2c with 3c and Fig. S4a with S4b).

2.4 **Droplet Size Affects Airborne Bacterial Viability**

To isolate the effects of different factors (such as solute concentration and droplet size) impacting airborne bacterial survival, the viability response of *E. coli* MRE162 levitated for 300s in droplets of LB broth with different initial solute concentrations equilibrating at 50%RH are compared in Fig. 4c.

The evaporation profiles of three different starting concentrations of non-metabolized LB broth are reported in Fig. 4a. The different initial concentrations lead to different equilibrated sizes although each achieves the same concentration of LB broth and moisture content when reaching an equilibrium at a specific RH (Fig. 4b), thereby having the same density. Thus, evaluation of solely the effect of different particle sizes containing the same solute concentration at equilibrium is possible. This is a unique and important element of this approach. The data in Fig. 4c suggests that either particle size and/or the dynamic processes during evaporation plays a crucial role in the survival response of *E. coli* MRE162.

3. DISCUSSION

The novel TAMBAS approach presented provides opportunity to explore the effect of individual parameters on airborne survival which could be crucial for fully understanding the fundamental mechanisms that control the transmission of airborne diseases. The ability to measure the impact of aerosol dynamics on the survival of microorganisms in the aerosol phase while reducing stresses involved in the generation, suspension and sampling processes is unique to this technique. Previous studies performed with evaporating sessile droplets (i.e. droplets deposited on surfaces) (52) or conventional technologies (53)(20) are often not representative of the natural mechanisms involved in the airborne transmission of disease. Therefore, data comparison becomes challenging due to the wide variety of methodologies, bioaerosol compositions and environmental conditions employed in longevity studies.

Supplementary Fig. S9 shows *E. coli* MRE162 viability at 300 s of suspension as a function of six different parameters (droplet cooling, volume reduction, surface to volume ratio, concentration of NaCl, concentration of solute and droplet volume) where only three (Figs. S9a, S9b and S9e) demonstrate a large collective correlation for both particle types (e.g. PBS and LB broth) reporting R^2 values of 0.78, 0.80 and 0.87 for droplet cooling, volume reduction and solute concentration,

respectively. These correlations of viability with droplet cooling, volume reduction and solute concentration, are all associated with the initial water mass flux from the droplet at the point of generation. Thus, although there is no apparent loss in viability during the drying phase (first 5-10 seconds), the impact of the initial mass flux from the droplet on microbe longevity, and overall change in size (Fig. 4), is consistent with an impact on viability over longer timescales. Put simply, the data suggest that the initial evaporation dynamics of the bioaerosol have a pronounced and predictable delayed effect on bioaerosol longevity and should be further explored. Ultimately this transformative approach will contribute to a more complete understanding of the fundamental factors influencing the airborne transmission of pathogens enabling development of refined hazard mitigation strategies.

4. MATERIALS AND METHODS

To demonstrate the utility of the new approach, *E. coli* MRE-162 was chosen as both a benchmark and a representative system to study bioaerosol. This bacteria strain presents a higher aerosol stability than other gram-negative bacteria and was proposed previously in the literature as a simulant for respiratory pathogens and to understand the effect of 'outdoor' conditions on survival. (54–58) In addition, wastewater treatment plants (WWTP) are a major emission source of bioaerosols due to the mechanical sewage treatment devices. *E. coli* has been detected in air sampled around such facilities and is known to cause zoonotic infection via aerosol route.(59)

4.1 Comprehensive Methodology for Bioaerosol Survival Studies

The TAMBAS approach was developed to elucidate the fundamental mechanisms responsible for degrading the viability of airborne microorganisms and, thus, to identify the parameters that define the transmission of airborne infection. The complementarity of two methodologies is used to resolve the complex interrelationship between the physicochemical and biological processes taking place from the production mechanism such as coughing and sneezing,(60) until the droplet reaches equilibrium and through to rehydration during the inhalation process. The CK-EDB method can be used to study the

evaporation/condensation kinetics, the solute hygroscopic properties and the evolving particle morphology during drying of single levitated aerosol particles.(37) These data can be used to develop a detailed understanding of the thermodynamic and kinetics processes that take place during the evaporation and condensation cycle occurring in a droplet lifespan. Additionally, the determination of survival rates of microorganism in populations of bioaerosol droplets as a function of atmospheric conditions, biological and chemical composition, and other biological factors such as the microbial concentration and physiology, can be performed with the novel CELEBS method.(25) An overview of both methodologies is included in the *Supplementary Information* (Table S1). Some of the key features accessible with this technique, enabling a detailed analysis of biological decay as a function of time, are: the suspension of particles in the true airborne state under a regulated atmosphere for a well-defined and unlimited period of time (~3 seconds to days) and with high time resolution (<1s); a quantifiable number of individual microbe containing droplets probed in each experiment; and control over the number of microbial cells hosted within each droplet. Importantly, the key elements of this methodology (e.g. the use of DoD generation to produce droplets of tailored composition, the imposition of low levels of charge on the particles to levitate particles) do not impact the viability of the microorganisms.(25) Details on the set-up, operation and data analysis of both methodologies are detailed below and in the Supplementary Figs S1 and S2.

Unique to this comprehensive methodology is the ability to combine our understanding of the microphysics and microbiology in the airborne state with time resolutions between 10 ms and 1s, respectively. Not only is the opportunity to achieve this in the aerosol phase, but the methodology allows us to investigate the repeatability and reproducibility for many droplets with the same desired initial conditions while minimizing stresses affecting microbial viability during aerosolisation, leading to low experimental uncertainties. This valuable alternative to conventional technologies will allow researchers to develop more accurate strategies to control the airborne transmission of disease.

4.2 Comparative Kinetics Methodology for Physicochemical Characterization of Bioaerosols

The ability to measure the dynamic behaviour of single levitated droplets using the concentric cylindrical electrodynamic balance (EDB) has been discussed in the literature.(27) A sample solution of known chemical and biological composition is introduced in the reservoir of a droplet-on-demand micro-dispenser (DoD) (Microfab MJ-ABP-01, 30 μm orifice). Single droplets are generated with a high level of size reproducibility (Supplementary Fig. S5) by applying a pulse voltage to the piezoelectric tip of the DoD and a small net charge is induced during droplet formation employing a high-voltage induction electrode located 2-3 mm from the tip of the DoD, allowing the droplet to be manipulated in the EDB. Approximately 100 ms after generation, the droplet is confined in the null point of the electrodynamic field where a 200 mL/min gas inlet at a temperature of 20°C regulates the RH (from 10 to 90%) inside the CK-EDB chamber by altering the mixing ratio of humidified and dry nitrogen flows. The trapped droplet is illuminated with a laser beam (Laser Quantum, Ventus continuous wave, CW) of wavelength λ=532 nm, and a CCD camera (Thorlabs) records the light scattering pattern, referred to as "phase function", at a central viewing angle of 45° every ~10 ms. By using the Geometrics Optics Approximation, the angular separation between light scattering fringes, $\Delta\vartheta$, in the phase function pattern is used to determine the absolute radius of the droplet(27) as a function of time together with the droplet morphology.(37)The droplet radius is estimated from the expression:(61)

$$r = \frac{\lambda}{\Delta\vartheta}\left(\cos\left(\frac{\vartheta}{2}\right) + \frac{n\ \sin\left(\frac{\vartheta}{2}\right)}{\sqrt{1+n^2-2n\cos\left(\frac{\vartheta}{2}\right)}}\right)^{-1} \quad (1)$$

where r is the radius of the droplet, ϑ is the central viewing angle and n is the droplet refractive index (RI) which is initially set as a constant value. In a post-analysis process, the variation in the droplet RI

with the mass fraction of solute (mfs) during evaporation is accounted for by applying a solute RI parametrisation generated by using the molar refraction mixing rule.(62) This revision process is repeated over 2-3 iterations until the radii and corresponding refractive indices values converge, providing accurate data for the droplet radius.(29)

From the droplet evaporation measurements, the hygroscopic growth properties at the thermodynamic equilibrium can be retrieved by using a comparative kinetics approach described in the literature and the section below.(29) Finally, the hygroscopicity data derived from the above process can be used to predict the evaporation dynamics for droplets of any size, composition, gas-phase RH and temperature. (26)

4.2.1 Determination of Droplet Hygroscopicity Properties

A comparative kinetics approach described in previous publications is used to retrieve the hygroscopic equilibrium response of solution droplets.(27, 37, 63) Specifically, sequences of ten pairs of probe and sample droplets with a different chemical composition are sequentially dispensed by two DoD micro-dispensers. Firstly, the evaporation profile of a probe droplet (a well-known systems such as water or aqueous NaCl solutions) is used to accurately determine the RH of the trapping atmosphere. Secondly, measurements of the corrected radius over time of the sample droplet is converted into mass by using a density parametrization. From these data, the mass flux as a function of time is calculated and used to determine the water activity at the droplet surface by using the mass and heat transport equation of Kulmala et al.(46) Finally, the droplet hygroscopicity is represented as the variation in mfs (calculated from the initial size and droplet composition) against the variation in water activity, providing the whole hygroscopicity curve.

4.2.2 Simulations of Droplet Evaporation Kinetics

Once the hygroscopic properties of the sample droplet are determined, it is possible to develop a solute hygroscopicity parametrization by using the equation developed by Kreidenweis et al.(64) which is

then introduced in the Kulmala model together with the density treatment of the solution droplet to generate predictions of mass-transfer kinetics for any initial solute concentration, droplet size and gas-phase RH and temperatures. Simulations resulting from this approach have shown an excellent agreement with experimental data. Associated errors with the thermodynamic predictions have been also discussed in previous work.(26) The possibility to build models that enable the prediction of evaporation kinetics of aerosol droplets containing microorganisms as a function of the initial droplet radius and composition allows further exploration of the interplay between all the physiochemical parameters affecting airborne bacteria survival (Supplementary Fig. S8).

4.2.3 Inferring Particle Morphology from the Light Scattering Pattern

The same light scattering pattern employed in the estimation of the droplet size has been also used to qualitatively infer the morphology of single levitated particles.(65, 66) Based on qualitative characteristics of the phase function, a new semi-quantitative methodology to differentiate among four main particle structures has been recently developed.(37) This robust approach relies on over one million observations of individual light scattering patterns to develop an algorithm which categorizes the particle morphology as homogeneous, a core-shell structure, a particle-containing inclusions or as a crystal or inhomogeneous particle. Specifically, an homogeneous and spherical evaporating droplet produces a regular and smooth evolution in its light scattering pattern which is characterised by equally spaced peaks. In the case of droplets containing inclusions, the regularity in the space between the peaks is maintained, however the intensity pattern can be randomly enhanced or reduced depending on the location of the inclusions within the droplet volume. In the evaporation of a droplet containing inclusions, the absolute number of inclusions remains constant and is determined based on the initial concentration pipetted on the DoD. However, the concentration of inclusions increases over time as water evaporates. The sensitivity of this method for the detection of inclusion within a particle is determined by their concentration. The absolute number of inclusions and their size were shown to be irrelevant in the determination of the lower detection limit.(37) The phase function for droplets within

a concentration gradient or core-shell structure is characterised by an additional envelope of intensity modulation superimposed on the regular fringes observed from a spherical particle due to the presence of a secondary structure. Finally, irregular or crystal particles report a highly irregular phase function over time which makes the determination of the particle size impossible. The sphere-equivalent size can be inferred from the size and solute concentration of the initial droplet. The ability to detect different morphologies on an individual bioaerosol droplet allows the possibility to explore the impact of particle phase and structure on microbial viability.

4.3 Levitation and Sampling Methodology for Biophysical Characterization of Bioaerosols

The ability to determine the biological decay rates of bioaerosols as a function of time, atmospheric conditions and chemical and biological composition has been recently developed.(25) The CELEBS apparatus is an adaptation of the double-ring electrodynamic trap(67) with important modifications that enable the generation, levitation and sampling of populations of bioaerosol droplets while minimizing the stresses associated with these processes when using conventional techniques for bioaerosol studies.(68, 69) All components are enclosed in a 3D printed chamber to avoid the disturbance of the levitated particles in a conditioned environment. CELEBS utilizes the same method of droplet generation used in the CK-EDB with the difference that in this case, a population of droplets is generated. A high-voltage induction electrode induces a small net charge on each particle allowing the population of droplets to be trapped in the electrodynamic field generated by applying an AC voltage (1000-2700V) to the two parallel ring electrodes located in the centre of the chamber. The net like-charge on all particles prevents coalescence among the population of droplets. The particles are confined in the electrodynamic field with a gas inlet, which enables the control of the atmospheric conditions (i.e. temperature, RH, gas, etc) inside the chamber and a 580 nm LED light illuminates the population of droplets allowing particle enumeration by using a LabView program developed in-house.

A probe connected to the gas inlet registers the %RH and temperature that the droplets are exposed to at every time. After the desired levitation period, the shielding on the sampling area is removed by retracting a safety plate. Then, the particles are extracted from the EDT onto the substrate holder by gradually reducing the amplitude of the waveform applied to the electrodes. The CELEBS instrument provides a 100% efficiency in the collection of the levitated particles by utilizing similar sampling velocities to the ones used with electrostatic precipitators,(70) consequently reducing the stresses associated with conventional bioaerosol samplers such as impingers.(24, 71) In addition, this methodology presents the possibility to probe viability/infectivity in any type of substrate (i.e. lung cells, microbiological media, ATP assays, etc). In this work, the bioaerosol droplets were sampled onto Petri dishes containing a ~3mm layer of LB agar and 300 µL volume of LB broth located in the centre of the plate. Finally, the Petri dishes were removed from the instrument, the LB broth containing the sampled bioaerosol was spread over the agar surface and the plates were incubated during 24h at 37°C. The approach used to calculate the survival rates of bacteria was previously described by us(25) and is also included in the SI.

4.3.1 Measurements of Survival Rate

The characterization of bioaerosol survival rates has been described in our previous work.(25) The loss of viability of airborne pathogens is represented as a reduction in their ability to form colony-forming units (CFUs) on plating media (culturability) as a function of time in the aerosol phase by using the following equation:

$$BD = \frac{C_{culturable}(TEST)}{C_{culturable}(CONTROL)} \times 100 \quad (5)$$

Where $C_{culturable}$ *(TEST)* is the number of CFUs obtained after the incubation of the bioaerosol population that was levitated for a set time interval. This measurement is normalized by using a $C_{culturable}$ *(CONTROL)* measurement to facilitate data comparison. Two options are valid as control

measurements: one is the absolute number of bacteria cells contained in the droplets estimated from the bacterial concentration introduced into the DoD. The second option is to measure the number of culturable cells (CFUs/droplet) obtained after a levitation time under 7 s in a preceding measurement. In this case, the levitation period is too brief to impact the viability of the microorganisms and therefore is considered as a non-exposure measurement. The validation of this assumption has been confirmed by comparing a series of CFUs/droplet obtained after 5 s "harmless" levitations with the original CFUs/droplet estimated by using the concentration of the cell suspension pipetted in the DoD.(25)

5. ACKNOWLEDGEMENTS

The authors acknowledge the contribution of the Natural Environment Research (NCAS-NERC) council and the Defence Science & Technology Laboratories (Dstl) for financial support through studentship funding. We acknowledge Jean-Charles Eloi, Electron Microscopy Technician in the School of Chemistry at the University of Bristol for his contribution in acquiring the SEM images used in this study. RJT recognises funding contributed by the UK Ministry of Defence.

6. AUTHOR CONTRIBUTIONS

A.E.H and M.O developed the approach with support from J.P.R, R.J.T and H.O. A.E.H and J.P.R. conceived and designed the project. M.O carried out the data analysis, wrote the paper, assisted to the design and development of the methodology and performed the laboratory work with support from A.E.H, R.J.T and H.O. A.E.H and J.P.R. are joint corresponding authors, supervised and coordinated the research and edited the manuscript for publication. J.P.R acquired funding and administered the project.

7. CONFLICTS OF INTEREST

The authors declare they have no conflicts of interest.

8. REFERENCES

1. Stilianakis NI, Drossinos Y. 2010. Dynamics of infectious disease transmission by inhalable respiratory droplets. J R Soc Interface 7:1355–1366.

2. Han ZY, Weng WG, Huang QY. 2013. Characterizations of particle size distribution of the droplets exhaled by sneeze. J R Soc Interface 10:20130560.

3. Sze To GN, Wan MP, Chao CYH, Fang L, Melikov A. 2009. Experimental study of dispersion and deposition of expiratory aerosols in aircraft cabins and impact on infectious disease transmission. Aerosol Sci Technol 43:466–485.

4. Wan MP, Sze To GN, Chao CYH, Wan MP, Fang L, Melikov A. 2009. Modeling the fate of expiratory aerosols and the associated infection risk in an aircraft cabin environment. Aerosol Sci Technol 43:322–343.

5. Douwes J, Thorne P, Pearce N, Heederik D. 2003. Bioaerosol health effects and exposure assessment: Progress and prospects. Ann Occup Hyg 47:187–200.

6. Morawska L, Cao J. 2020. Airborne transmission of SARS-CoV-2 : The world should face the reality. Environ Int 139:105730.

7. Haddrell AE, Thomas RJ. 2017. Aerobiology: Experimental considerations, observations, and future tools. Appl Environ Microbiol 83:1–17.

8. Marr LC, Tang JW, Van Mullekom J, Lakdawala SS. 2019. Mechanistic insights into the effect of humidity on airborne influenza virus survival, transmission and incidence. J R Soc Interface 16:20180298.

9. Kukavica-Ibrulj I, Levesque RC. 2008. Animal models of chronic lung infection with Pseudomonas aeruginosa: useful tools for cystic fibrosis studies. Lab Anim 42:389–412.

10. Du P, Du R, Ren W, Lu Z, Fu P. 2018. Seasonal variation characteristic of inhalable microbial

communities in PM 2.5 in Beijing city, China. Sci Total Environ 610–611:308–315.

11. Dunklin EW, Puck TT. 1948. The lethal effect of relative humidity on air-borne bacteria. Public Health 87,2:87–101.

12. Benbough JE. 1967. Death mechanisms in airborne Escherichia coli. J Gen Microbiol 47:325–333.

13. Webb SJ. 1959. Factors affecting the viability of air-borne bacteria. Can J Microbiol 14:742–745.

14. Lighthart B, Shaffer BT, Lighthart* B, Shaffer BT. 1997. Increased Airborne Bacterial Survival as a Function of Particle Content and Size. Aerosol Sci Technol 27:439–446.

15. Jones AM, Harrison RM. 2004. The effects of meteorological factors on atmospheric bioaerosol concentrations - A review. Sci Total Environ 326:151–180.

16. Davis MS, Bateman JB. 1960. Relative humidity and the killing of bacteria. I. Observations on Escherichia coli and Micrococcus lysodeikticus. J Bacteriol 80:577–579.

17. Cox CS, Goldberg LJ. 1972. Aerosol survival of Pasteurella tularensis and the influence of relative humidity. Appl Microbiol 23:1–3.

18. Benbough JE. 1971. Some Factors Affecting the Survival of Airborne Viruses. J gen Virol 10:209–220.

19. Ehrlich R, Miller S, Walker RL. 1970. Relationship between atmospheric temperature and survival of airborne bacteria. Appl Microbiol 19:245–249.

20. Fernstrom A, Goldblatt M. 2013. Aerobiology and its role in the transmission of infectious diseases. J Pathog 2013:493960.

21. Gralton J, Tovey E, McLaws ML, Rawlinson WD. 2011. The role of particle size in aerosolised pathogen transmission: A review. J Infect 62:1–13.

22. Alsved M, Bourouiba L, Duchaine C, Löndahl J, Marr LC, Parker ST, Prussin AJ, Thomas RJ. 2019. Natural sources and experimental generation of bioaerosols: Challenges and perspectives. Aerosol Sci Technol 0:1–25.

23. Zhen H, Han T, Fennell DE, Mainelis G. 2014. A systematic comparison of four bioaerosol generators: Affect on culturability and cell membrane integrity when aerosolizing Escherichia coli bacteria. J Aerosol Sci 70:67–79.

24. Dabisch P, Bower K, Dorsey B, Wronka L. 2012. Recovery efficiencies for *Burkholderia thailandensis* from various aerosol sampling media. Front Cell Infect Microbiol 2:78.

25. Otero-Fernandez M, Thomas RJ, Garton NJ, Hudson A, Haddrell A, Reid JP. 2019. Assessing the airborne survival of bacteria in populations of aerosol droplets with a novel technology. J R Soc Interface 16:20180779.

26. Davies JF, Haddrell AE, Rickards AMJ, Reid JP. 2013. Simultaneous analysis of the equilibrium hygroscopicity and water transport kinetics of liquid aerosol. Anal Chem 85:5819–5826.

27. Davies JF, Haddrell AE, Reid JP. 2012. Time-resolved measurements of the evaporation of volatile components from single aerosol droplets. Aerosol Sci Technol 46:666–677.

28. Power RM, Simpson SH, Reid JP, Hudson AJ. 2013. The transition from liquid to solid-like behaviour in ultrahigh viscosity aerosol particles. Chem Sci 4:2597.

29. Rovelli G, Miles REH, Reid JP, Clegg SL. 2016. Accurate Measurements of Aerosol Hygroscopic Growth over a Wide Range in Relative Humidity. J Phys Chem A 120:4376–4388.

30. Carslaw KS, Clegg SL, Brimblecombe P. 1995. A Thermodynamic Model of the System HCl-HNO3-H2SO4-H2O, Including Solubilities of HBr, from <200 to 328 K. J Phys Chem 99:11557–11574.

498 31. Goldberg LJ, Watkins HMS, Boeeke EE. 1958. The use of a rotating drum for the study of
499 aerosols over extended periods of time 58:85–93.

500 32. Cox CS, Gagen SJ. 1974. Aerosol survival of Sevvatia marcescens as a function of oxygen
501 concentration, relative humidity, and time 20:1529–1534.

502 33. Cox CS. 1971. Aerosol survival of Pasteurella tularensis disseminated from the wet and dry
503 states. Appl Microbiol 21:482–486.

504 34. Donaldson AI, Ferris NP. 1975. The Survival of Foot-and-Mouth Disease Virus in Open Air
505 Conditions. J Hyg (Lond) 74:409–416.

506 35. Lever MS, Williams A, Bennett AM. 2000. Survival of mycobacterial species in aerosols
507 generated from artificial saliva. Lett Appl Microbiol 31:238–241.

508 36. Zuo Z, Kuehn TH, Bekele AZ, Mor SK, Verma H, Goyal SM, Raynor PC, Pui DYH. 2014.
509 Survival of airborne MS2 bacteriophage generated from human saliva, artificial saliva, and cell
510 culture medium. Appl Environ Microbiol 80:2796–2803.

511 37. Haddrell A, Rovelli G, Lewis D, Church T, Reid J, Haddrell A, Rovelli G, Lewis D, Church T.
512 2019. Identifying time-dependent changes in the morphology of an individual aerosol particle
513 from its light scattering pattern. Aerosol Sci Technol 0:1–18.

514 38. Davies JF, Haddrell AE, Miles REH, Bull CR, Reid JP. 2012. Bulk, surface, and gas-phase
515 limited water transport in aerosol. J Phys Chem A 116:10987–10998.

516 39. Bones DL, Reid JP, Lienhard DM, Krieger UK. 2012. Comparing the mechanism of water
517 condensation and evaporation in glassy aerosol. Proc Natl Acad Sci U S A 109:11613–11618.

518 40. Goto M, Oaki Y, Imai H. 2016. Dendritic growth of NaCl crystals in a gel matrix: Variation of
519 branching and control of bending. Cryst Growth Des 16:4278–4284.

520 41. Gregson FKA, Robinson JF, Miles REH, Royall CP, Reid JP. 2019. Drying Kinetics of Salt

Solution Droplets: Water Evaporation Rates and Crystallization. J Phys Chem B 123:266–276.

42. Yang W, Marr LC. 2012. Mechanisms by which ambient humidity may affect viruses in aerosols. Appl Environ Microbiol 78:6781–6788.

43. Haddrell AE, Hargreaves G, Davies JF, Reid JP. 2013. Control over hygroscopic growth of saline aqueous aerosol using Pluronic polymer additives. Int J Pharm 443:183–192.

44. Power RM, Reid JP. 2014. Probing the micro-rheological properties of aerosol particles using optical tweezers. Reports Prog Phys 77:074601.

45. Girod M, Moyano E, Campbell DI, Cooks RG. 2011. Accelerated bimolecular reactions in microdroplets studied by desorption electrospray ionization mass spectrometry. Chem Sci 2:501–510.

46. Kulmala M, Vesala T, Wagner PE. 1993. An Analytical Expression For the Rate of Binary Condensational Particle Growth. Proc R Soc A Math Phys Eng Sci 441:589–605.

47. Ferry RM, Brown WF, Damon EB. 1958. Studies of the loss of viability of bacterial aerosols: III. Factors affecting death rates of certain Non-Pathogens. J Hyg (Lond) 56:389–403.

48. Ferry RM, Brown WF, Damon EB. 1958. Studies of the loss of viability of stored bacterial aerosols. II. Death rates of several non-pathogenic organisms in relation to biological and structural characteristics. J Hyg (Lond) 56:125–150.

49. Scott WJ. 1958. The effect of residual water on the survival of dried bacteria during storage. J Gen Microbiol 19:624–633.

50. Ferry RM, Maple TG. 1954. Studies of the loss of viability of stored bacterial aerosols. I. Micrococcus candidus. J Infect Dis 95:142–159.

51. Cai C, Stewart DJ, Reid JP, Zhang YH, Ohm P, Dutcher CS, Clegg SL. 2015. Organic component vapor pressures and hygroscopicities of aqueous aerosol measured by optical

tweezers. J Phys Chem A 119:704–718.

52. Vejerano EP, Marr LC. 2018. Physico-chemical characteristics of evaporating respiratory fluid droplets. J R Soc Interface 15:1–10.

53. Willem L, van Kerckhove K, Chao DL, Hens N, Beutels P. 2012. A Nice Day for an Infection? Weather Conditions and Social Contact Patterns Relevant to Influenza Transmission. PLoS One 7.

54. Ng TW, Chan WL, Lai KM. 2017. Importance of stress-response genes to the survival of airborne Escherichia coli under different levels of relative humidity. AMB Express 7:71.

55. Lin K, Marr LC. 2020. Humidity-Dependent Decay of Viruses, but Not Bacteria, in Aerosols and Droplets Follows Disinfection Kinetics. Environ Sci Technol 54:1024–1032.

56. Dybwad M, Skogan G. 2017. Aerobiological Stabilities of Different Cell Clusters of Different Compositions 83:1–12.

57. de Mik G, de Groot I. 1977. The germicidal effect of the open air in different parts of The Netherlands 78:175–187.

58. Benbough JE, Hambleton P, Martin KL, Strange RE. 1972. Effect of aerosolization on the transport of -methyl glucoside and galactosides into Escherichia coli. J Gen Microbiol 72:511–520.

59. Vantarakis A, Paparrodopoulos S, Kokkinos P, Vantarakis G, Fragou K, Detorakis I. 2016. Impact on the Quality of Life When Living Close to a Municipal Wastewater Treatment Plant. J Environ Public Health 2016.

60. Johnson GR, Morawska L, Ristovski ZD, Hargreaves M, Mengersen K, Chao CYH, Wan MP, Li Y, Xie X, Katoshevski D, Corbett S. 2011. Modality of human expired aerosol size distributions. J Aerosol Sci 42:839–851.

567 61. Glantschnig WJ, Chen S-H. 1981. Light scattering from water droplets in the geometrical optics
568 approximation. Appl Opt 20:2499.

569 62. Cai C, Miles REHH, Cotterell MI, Marsh A, Rovelli G, Rickards AMJJ, Zhang YH, Reid JP.
570 2016. Comparison of methods for predicting the compositional dependence of the density and
571 refractive index of organic-aqueous aerosols. J Phys Chem A 120:6604–6617.

572 63. Rovelli G, Miles EHR, Reid PJ, Clegg LS. 2017. Hygroscopic properties of aminium sulfate
573 aerosols. Atmos Chem Phys 17:4369–4385.

574 64. Kreidenweis SM, Koehler K, DeMott PJ, Prenni AJ, Carrico C, Ervens B. 2005. Water activity
575 and activation diameters from hygroscopicity data - Part I: Theory and application to inorganic
576 salts. Atmos Chem Phys 5:1357–1370.

577 65. Archer J, Kolwas M, Jakubczyk D, Derkachov G, Woźniak M, Kolwas K. 2017. Evolution of
578 radius and light scattering properties of single drying microdroplets of colloidal suspension. J
579 Quant Spectrosc Radiat Transf 202:168–175.

580 66. Krieger UK, Meier P. 2011. Observations and calculations of two-dimensional angular optical
581 scattering (TAOS) patterns of a single levitated cluster of two and four microspheres. J Quant
582 Spectrosc Radiat Transf 112:1761–1765.

583 67. Davis EJ. 1997. A history of single aerosol particle levitation. Aerosol Sci Technol 26:212–254.

584 68. Thomas RJ, Webber D, Hopkins R, Frost A, Laws T, Jayasekera PN, Atkins T. 2011. The cell
585 membrane as a major site of damage during aerosolization of Escherichia coli. Appl Environ
586 Microbiol 77:920–925.

587 69. Terzieva S, Donnelly J, Ulevicius V, Grinshpun SA, Willeke K, Stelma GN, Brenner KP. 1996.
588 Comparison of methods for detection and enumeration of airborne microorganisms collected by
589 liquid impingement. Appl Environ Microbiol 62:2264–2272.

590 70. Mainelis G, Adhikari A, Willeke K, Lee SA, Reponen T, Grinshpun SA. 2002. Collection of
591 airborne microorganisms by a new electrostatic precipitator. J Aerosol Sci 33:1417–1432.

592 71. Juozaitis A, Willeke K, Grinshpun SA, Donnelly J. 1994. Impaction onto a glass slide or agar
593 versus impingement into a liquid for the collection and recovery of airborne microorganisms.
594 Appl Environ Microbiol 60:861–870.

595

596

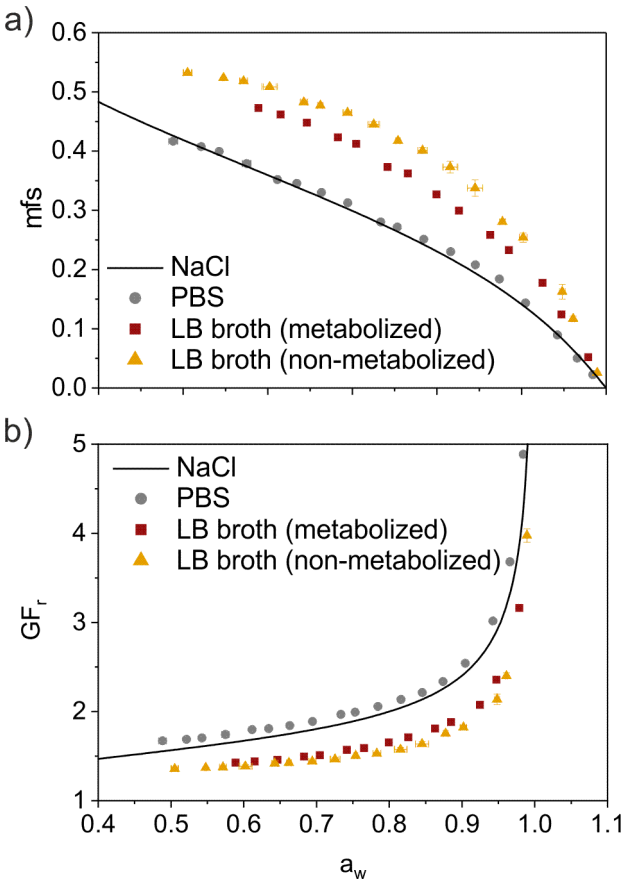

597

598 **Figure 1.** Hygroscopicity curves of different culture media with variation in solution water activity
599 (a_w), presented in terms of (a) mass fraction of solute (mfs) and (b) radial growth factor (GF_m).
600 Predicted curves for NaCl hygroscopicity (line) from the E-AIM model are also shown for reference.

601

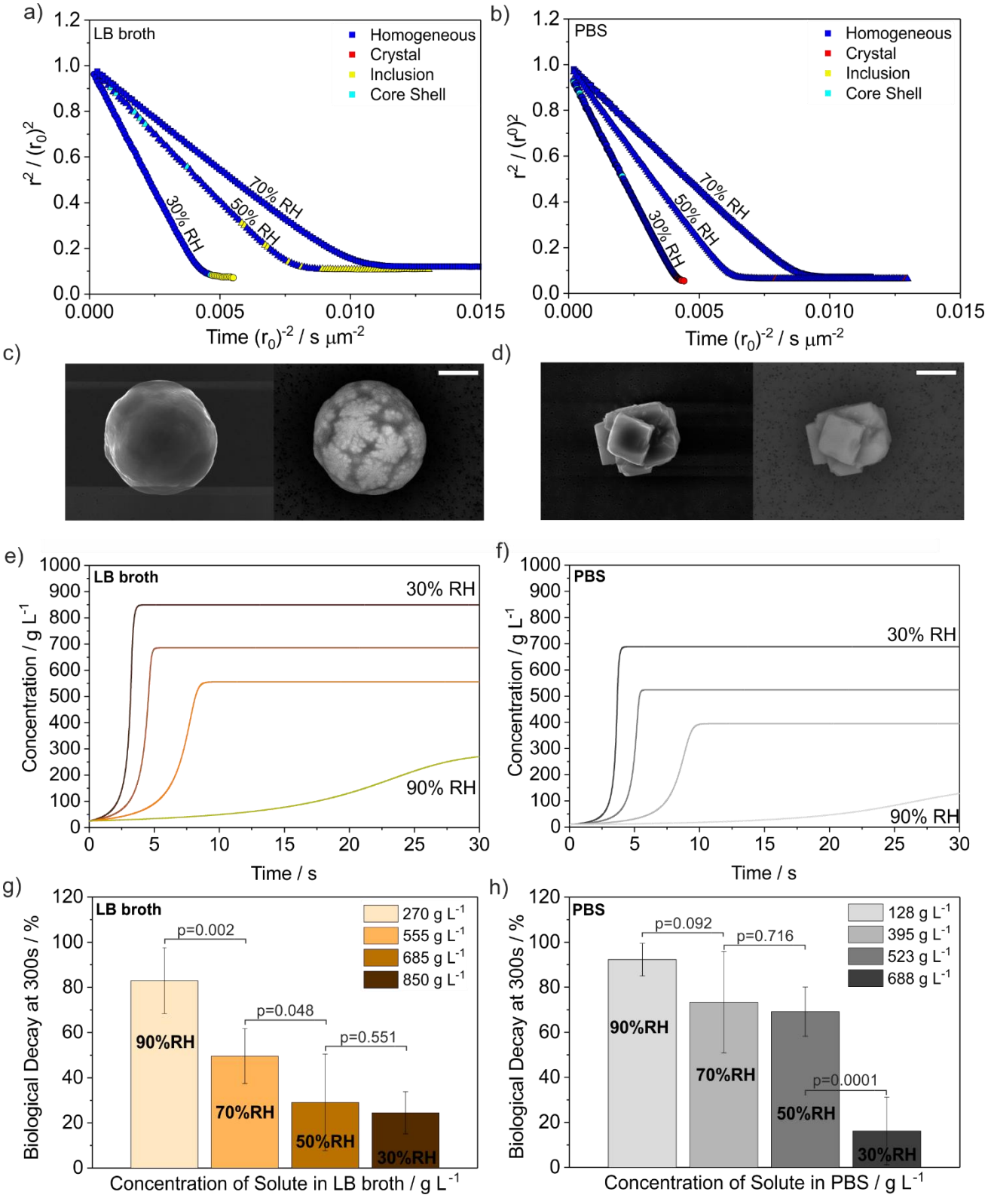

Figure 2. Evolution of size and morphology for evaporating droplets of (a) non-metabolized LB broth, (b) PBS into 30%, 50% and 70% gas-phase RHs. Slopes for the linear trend in the radius-squared are -216.7, -118.1 and -90.4 in the case of LB broth droplets and -221.9, -153.4 and -108.7 for PBS droplet

composition, each at 30, 50 and 70% RHs, respectively. SEM and backscattered electron images for particles formed from (c) non-metabolized LB broth and (d) PBS at 30% RH are shown. Predicted time-dependent solute concentrations for evaporation of droplets into RHs spanning from 30 to 90% RHs and 20 ℃ for droplets solutions of (e) non-metabolized LB broth and (f) PBS are shown. To simulate the evaporation profiles, a starting radius of 25 μm and concentration of 25 g L^{-1} and 9.5 g L^{-1} for LB broth and PBS were used, respectively. The impact of morphology and solute concentration on airborne bacteria viability at 300 s from droplet generation and at RHs of 30 to 90% RH are shown for (g) LB broth and (h) PBS droplets containing *E. coli* MRE162 (starting concentration of $(2.6\pm0.6)\times10^{8}$ CFU ml^{-1}, 28±11 CFUs $droplet^{-1}$). *p*-values obtained when comparing LB broth and PBS compositions at 90, 70, 50 and 30% RHs by applying a two-sample t-test are 0.137, 0.079, 0.00 and 0.22, respectively, showing only a significant difference on survivability between compositions at 50% RH.

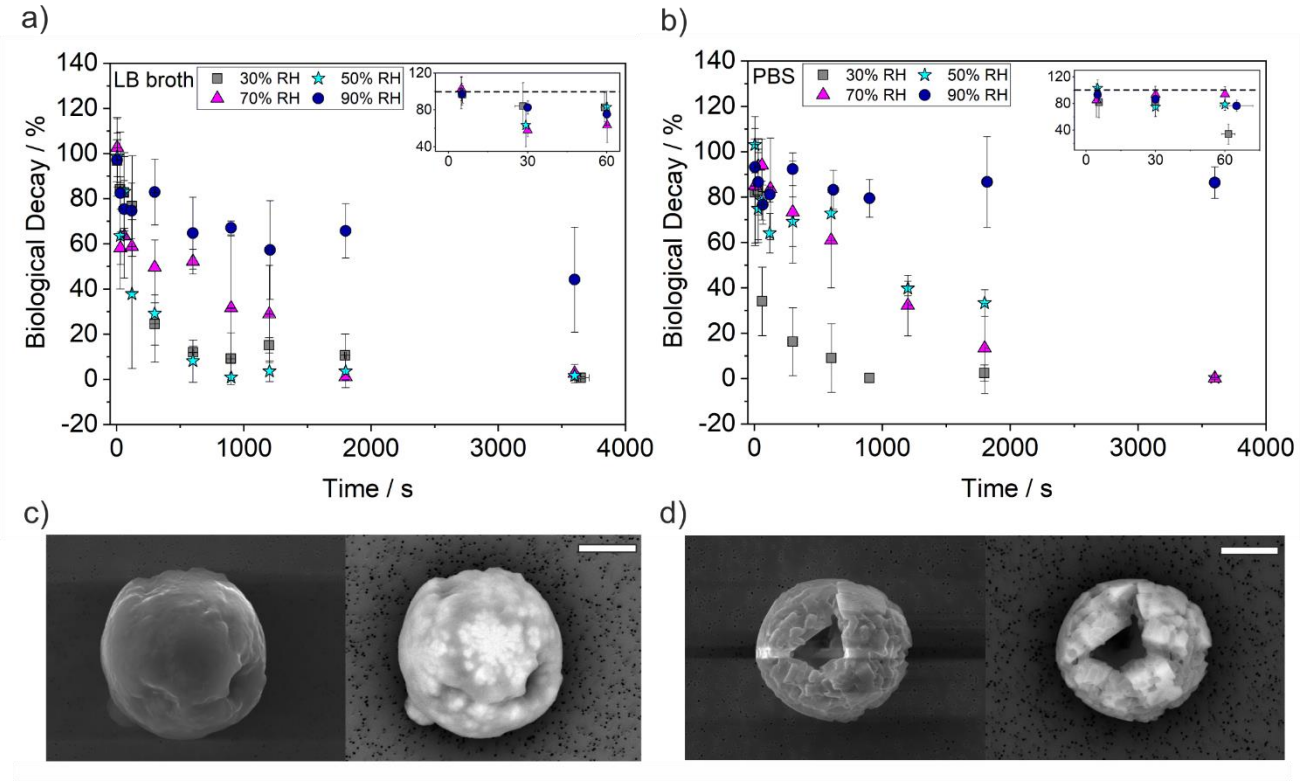

Figure 3. Relationship between solute compositions on bacteria airborne survival as a function of RH and survival for *E. coli* MRE162 (2.6±0.6 10^8 CFU ml^{-1}) in (a) LB broth and (b) PBS droplets. Note that in (b), the data points for 50% and 70%RH at 3600s overlap. Insets show the survival decay during a timeframe of 60 s levitation. SEM and backscattered electron images for (c) LB broth and (d) PBS droplets containing *E. coli* MRE-162 at (2.6±0.6) $\times 10^9$ CFU ml^{-1} at 30% RH. Scale bars represent 5 μm.

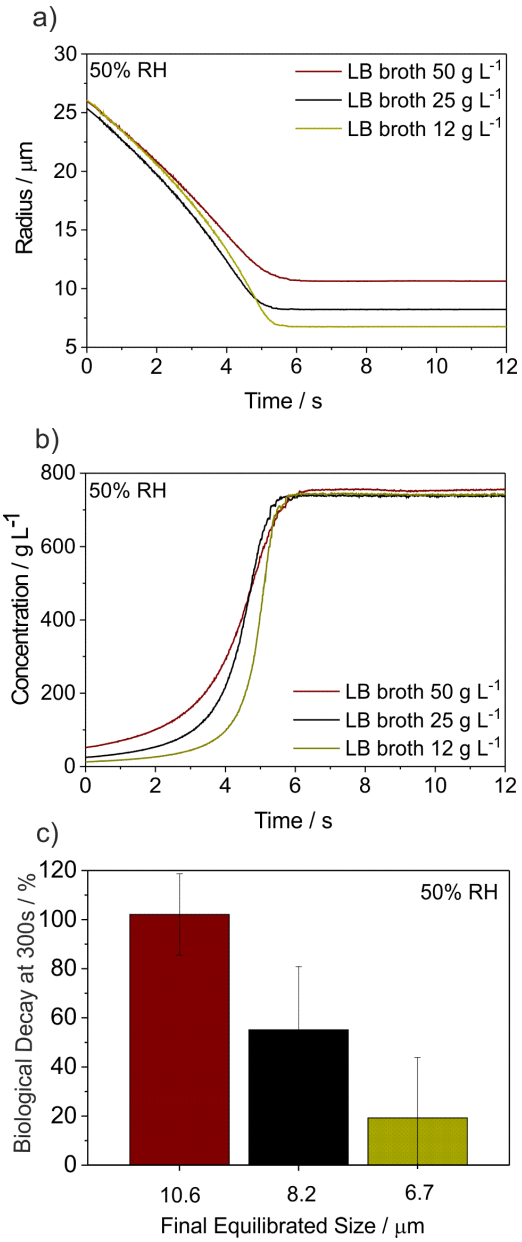

628

629 **Figure 4.** (a) Comparison of the measured (a) particle size and (b) changes in solute concentration (g
630 L^{-1}) of LB broth droplets with different initial solute concentrations evaporating into 50% RH and
631 20 ℃. (c) The effect of the equilibrium particle size on bacteria viability. All the survivability data are
632 expressed as the average and standard deviation for three replicates per experiment were populations
633 from 2 to 6 droplets were levitated.

634